Imaging Water Dissociation on TiO_2(110): Evidence for Inequivalent Geminate OH Groups

Z. Zhang,[†,‡] O. Bondarchuk,[†] Bruce D. Kay,[‡] J. M. White,*[,†,§] and Z. Dohnálek*[,‡]

Department of Chemistry and Biochemistry, Center for Materials Chemistry, University of Texas at Austin, Texas 78712, and Fundamental Sciences Directorate and Institute for Interfacial Catalysis, Pacific Northwest National Laboratory, Richland, Washington 99352

Received: June 9, 2006; In Final Form: August 16, 2006

Identical regions of partially reduced TiO_2(110) surfaces with bridge-bonded oxygen vacancy (BBO_V) concentrations of ∼10% ML (1 ML = 5.2×10^{14} cm^{-2}) were imaged using scanning tunneling microscopy (STM) before and after dosing H_2O at ambient temperature (∼300 K). Atomically resolved images confirm that H_2O adsorbs dissociatively on the BBO_V sites, producing two hydroxyl species, one positioned at BBO_V and denoted OH_V and the other, denoted OH_B, formed by protonation at either of the two nearest-neighbor bridge-bonded oxygen atoms. Hydrogen hopping along the [001] direction is observed at ambient temperature, with a strong preference for OH_B (∼10×) hydrogen motion. This powerful imbalance demonstrates the inequality of OH_V and OH_B and suggests differences in their charge and/or binding configuration.

1. Introduction

The TiO_2-H_2O system is of great interest for many areas of both fundamental and applied science, including photocatalysis, electrochemistry, active coatings, and corrosion.[1,2] For example, the discovery of photochemical water dissociation on TiO_2, with potential applications in solar cells,[3] has stimulated extensive research on reactions of water on titania surfaces. In particular, the detailed understanding of water adsorption, diffusion, and dissociation on prototypical rutile TiO_2(110) has become one of the leading topics in the area of oxide surface chemistry.[4] The reactivity of rutile TiO_2(110) is believed to be dominated by missing oxygen ion defect sites, generally called bridge-bonded oxygen vacancies (BBO_V's). Understanding the chemical activity of this particular surface site has become the focus of a number of model catalytic studies.[4,5] These sites are normally generated upon partial reduction of TiO_2(110) as O_2 is desorbed during high-temperature (∼900 K) sample preparation. Two electrons that are left behind lead to reduction of titanium ions near the vacancy into a formal (3+) oxidation state.[4,6] For H_2O, there is good evidence that dissociative adsorption is limited to BBO_V sites.[7−10] Upon dissociation, two OH groups are formed on the adjacent bridge-bonded sites along a single oxygen atom row. The spectroscopic evidence points to the fact that the defect oxidation state (Ti^{3+}) is preserved upon OH formation.[6,8,11] Annealing of the surface leads to recombination of two OH groups and formation of $H_2O_{(g)}$ and BBO_V at ∼450 K.[7,9]

Scanning tunneling microscopy (STM) offers the possibility to image the adsorption, dissociation, and diffusion of atoms and molecules on surfaces. Several groups have used STM to investigate the interaction of water with TiO_2(110).[10,12−14] Recently, two STM investigations reported direct imaging of water dissociation on BBO_V sites.[15,16] Paired hydroxyl groups located on two neighboring bridge-bonded oxygen (BBO) sites have been shown to result from direct water dissociation at oxygen vacancies. At low temperature (∼187 K), the mobile H_2O molecules adsorbed on Ti^{4+} rows were observed to induce hydrogen migration from one BBO row to another.[15] Similar adsorbate-assisted hydrogen migration across BBO rows was also observed in our investigation of methanol on TiO_2(110).[17] Surprisingly, direct hydrogen hopping along a single BBO row has not been reported to date, and the lack of mobility is attributed to an unusually high diffusion barrier of ∼1.5 eV.[14]

In this paper, we use STM to image and characterize the time evolution of OH groups formed upon H_2O dissociation on TiO_2-(110) BBO_V sites at very low coverages. We have confirmed that an adjacent hydroxyl pair, one member positioned at the BBO_V, denoted OH_V, and the other, denoted OH_B, formed by hydrogen addition to either of the two nearest-neighbor BBO atoms, is the direct product of water dissociation. At ∼300 K, the pairs separate via hydrogen hopping along the BBO row; this is ascribed to thermal activation and is unassisted by molecular H_2O. Remarkably, the hydrogen hop associated with the OH_V is observed roughly tenfold less frequently than its neighboring OH_B, conclusively demonstrating the chemical inequivalence of OH_V and OH_B at 300 K. This distinguishibility suggests that the charge (nominally $2e^-$) associated with the two underlying Ti^{3+} ions underneath a BBO_V is not symmetrically redistributed between the OH_B and OH_V pair and their underlying cations and/or that the OH_V is bound differently from OH_B. Heterolytic water dissociation into H^+ and OH^- may also be an important contributor to the differences. Thus, there are atomic and/or electronic structure differences at these two positions along the BBO row.

2. Experimental Section

Experiments were performed in an ultrahigh-vacuum chamber (base pressure $<8 \times 10^{-11}$ Torr) equipped with Omicron variable temperature STM, Auger electron spectroscopy (PHI), and quadrupole mass spectrometry (UTI). The TiO_2(110) ($10 \times 3 \times 1$ mm^3, Princeton Scientific) was mounted on a standard

* Corresponding authors. E-mail: Zdenek.Dohnalek@pnl.gov. E-mail: JMWhite@mail.utexas.edu.
[†] University of Texas at Austin.
[‡] Fundamental Sciences Directorate and Institute for Interfacial Catalysis.
[§] Institute for Interfacial Catalysis.

10.1021/jp063619h CCC: $33.50
Published on Web 10/04/2006

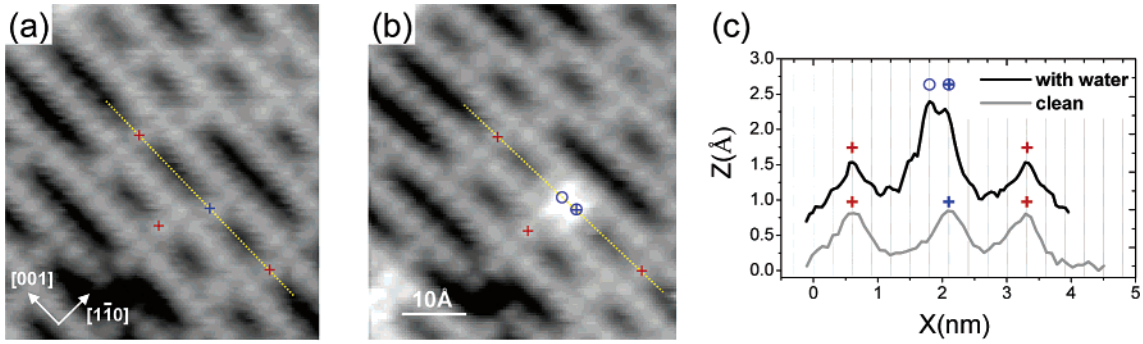

Figure 1. Two STM images obtained from the same area of TiO_2(110) before (a) and after (b) background adsorption of H_2O at RT (bias voltage, +0.4 V; tunneling current, 0.03 nA). The + signs mark the positions of several BBO_V's. Two circles (hatched, at the BBO_V position; open, adjacent to BBO_V) mark the positions of two OH groups formed after H_2O adsorption and dissociation on the BBO_V site. (c) Line profiles indicated in panels (a) and (b) before and after water adsorption along [001] direction. Vertical lines represent the bridge-bonded oxygen atom positions.

Omicron single-plate tantalum holder and heated radiatively with a tungsten filament heater located behind the sample plate. Prior to use, commercial STM tips (Tungsten, Custom Probe Unlimited) were cleaned via Ne sputtering and UHV annealing. The sample temperature dependence on heater power was calibrated in a separate experiment using a TiO_2(110) crystal with a chromel−alumel thermocouple glued directly to the crystal surface. Well-ordered TiO_2(110) surfaces were prepared using repeated cycles of Ne ion sputtering and UHV annealing at 900−1000 K. After cooling to 350−320 K, the clean sample was transferred to the STM stage and an area A_o (characterized by distinct "geographic" features such as surrounding steps) was immediately imaged. As expected, the time required to acquire the first image varied significantly (20−50 min) depending on the condition of the tip. Results from 8 separate experiments involving scanning for extended periods of time (up to 170 min) resulted in sequences of up to 107 images of the same surface area. Only representative subsets of data that illustrate the observed surface processes are presented.

Water was dosed from one of two sources—either through exposure to residual background H_2O or via a retractable tube doser with a 7-μm pinhole aperture. Using background H_2O (partial pressure $2-4 \times 10^{-11}$ Torr) was helpful in that the amount of dosed water could be easily kept below the BBO_V concentration (~10% ML) over the duration of the experiment. We found that the dissociation and diffusion process is the same for both dosing sources. When using the doser, the H_2O (Fisher, 99.9+ %) was purified by several freeze−pump−thaw cycles using liquid nitrogen. In this case, the W STM tip was retracted ~1 μm prior to dosing H_2O from the surface to avoid shadowing the imaged area. The end of the doser was positioned within 5 mm of the sample surface. After dosing, the tube doser was retracted and the STM tip moved to reimage area A_o. We find that, after the tip approach, water adsorption from the background on the scanned area proceeds significantly more slowly compared to other areas due to tip shadowing. This is clearly documented by imaging of other areas that are not affected by the tip at the end of the experiment. All STM images (empty states) were collected using constant-current (~0.1 nA) tunneling mode with a positive sample bias voltage (0.4−2.5 V) and processed using WSxM software (Nanotech, freeware).[18]

3. Results and Discussion

Figure 1 displays STM images of the same surface area, A_o, before, Figure 1a, and after, Figure 1b, adsorption of background H_2O at ambient temperature. The bright rows on Figure 1a are identified as the fivefold coordinated Ti^{4+} ions; the dark rows are the BBO ions.[4] The bright spots along the BBO rows are assigned to BBO_V's. With respect to the surface Ti^{4+}, the number density of BBO_V is 10 ± 1%. In accord with literature reports, the contrast in Figure 1a between the dark rows and the bright spots on the dark rows is, at most, weakly dependent on the bias voltage (+0.5 to 3 V).[13]

In Figure 1a, we mark (+) the positions of several BBO_V sites, one of which is altered in Figure 1b by water uptake from background. After water adsorption from background, Figure 1b, the intensity and position of all BBO_V's within A_o remain unchanged with respect to Figure 1a with one exception. One new, particularly bright feature, marked with two circles, is located at the position of one of the marked, original BBO_V's in Figure 1a. Images of larger areas (not shown) confirm that, as the H_2O exposure increases, equivalent features continue to appear at BBO_V positions. Unlike the bright spots associated with unfilled BBO_V's, the relative intensity of the filled vacancies depends strongly on the bias voltage.[13] In the experiment of Figure 1, a tip with extremely high resolution was prepared, yielding an image that resolves the OH groups on neighboring BBO sites (marked with two circles). More typically, this feature appears as one larger bright feature[14−16] centered between two neighboring BBO sites as discussed below in Figure 2.

We have further confirmed our assignments of OH by applying high-voltage pulses (data not shown). Consistent with literature reports,[13,14,17] filled vacancies—but not the BBO_V's—can be altered using biases exceeding 3 V. In this process, filled vacancy bright spots are removed, but the original BBO_V does not reappear. This is taken as an indication of tip-stimulated removal of H but not O.

Line scans along dark rows in the images in Figure 1a,b, scaled using high-resolution line scans along the Ti^{4+} rows, are helpful in identifying the spacing between vacancies and the location of filled vacancy features with respect to the substrate atoms. In Figure 1c, the vertical dashed gridlines correspond to the positions of the BBO atoms. The two curves in Figure 1c are line scans of identical segments along the [001] direction before and after dosing water from the background. Two of the three vacancies on the dotted line in Figure 1a remain unoccupied in Figure 1b, while the third is replaced by a broader higher-intensity region with two local maxima—one located at the original vacancy position (circle containing "+" in Figure 1b), and the other at the nearest-neighbor BBO position (open circle). The positions of the two local maxima provide direct evidence that water molecules dissociate upon adsorption on BBO_V's at ~300 K; the OH located at BBO_V is denoted OH_V, while that at the nearest-neighbor BBO is denoted OH_B. Were water adsorption at a BBO_V nondissociative, the tunneling

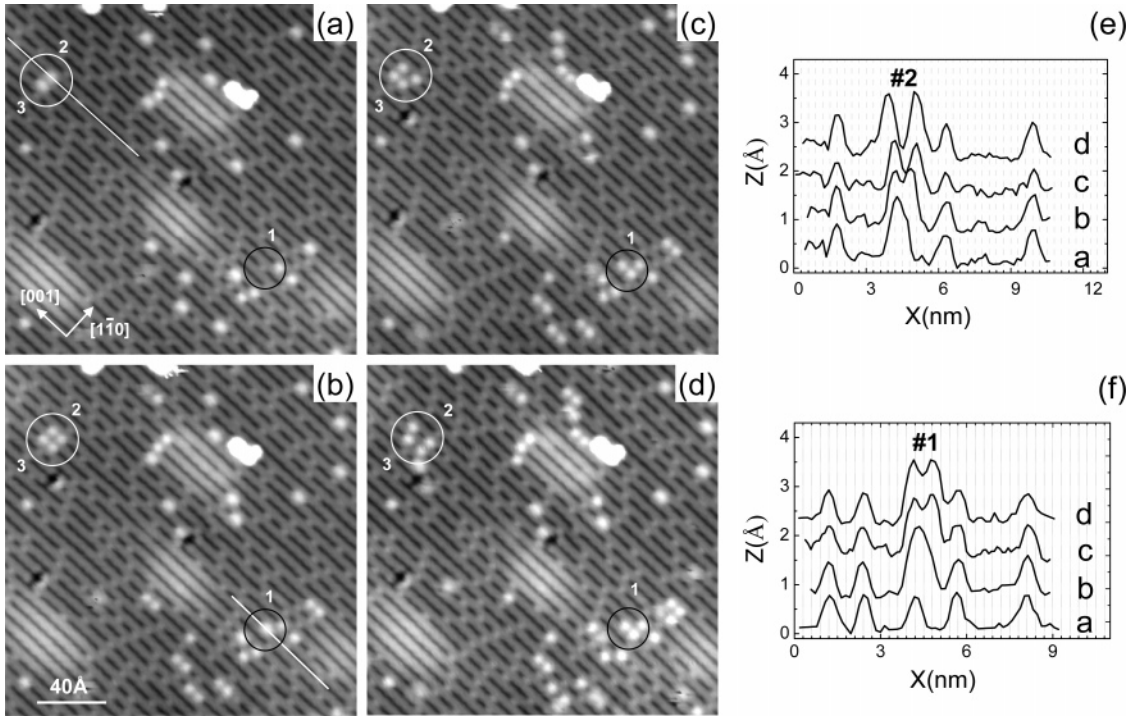

Figure 2. Sequential STM images (bias voltage, +2.5 V; tunneling current, 0.07 nA) recorded as a function of time on water-exposed TiO_2(110) with corresponding line profiles: (a) first image defined as 0 min; (b) 21 min later; (c) 35 min later; (d) 50 min later. (e) Line profiles along the [001] direction on hydroxyl pair #2 for the four scans from (a) to (d). (f) Line profiles along [001] direction on hydroxyl pair #1 (first appearing in (b)) for the four scans from (a) to (d). Vertical lines represent the bridge-bonded oxygen atom positions.

profile would be symmetrically, rather than asymmetrically, positioned with respect to the position of the vacancy. These STM results for very low doses of H_2O are consistent with and, via improved resolution, provide deeper insight than previous literature.[10,12−16]

In a separate experiment, H_2O was introduced via background dosing. Here, the first high-quality image was obtained relatively quickly, and the system was so stable that the same area was imaged for nearly an hour. The first image, Figure 2a, was collected 20 min after transferring a clean sample into the STM imaging position. In this image, most of the BBO_V's are not filled, indicating that the amount of H_2O dosed is much less than the BBO_V concentration. With respect to the image of Figure 2a, the time intervals, Δt, for the subsequent images were 21, 35, and 51 min (Figure 2b−d). The number of bright features increases slowly over this time interval; there are twice as many bright spots in Figure 2d as in Figure 2a. While most of the new features are due to separation of adjacent OH groups as further discussed below, some are also due to additional water adsorption, e.g., the bright spot labeled #1 in Figure 2b. It is important to note that total dissociative water accumulation over 70 min fills only a small fraction (ca. 10%) of the original BBO_V's. This accumulation of water is extremely slow and provides the necessary conditions for direct observation of hydrogen diffusion in the absence of molecular water as discussed below.

In comparison to Figure 1, the data presented in Figure 2 represent a more typical resolution obtained on TiO_2(110). In this case, the neighboring OH groups resulting from H_2O dissociation cannot be directly resolved, and they appear as a single bright feature centered on the BBO row and elongated along the [001] direction. Two such hydroxyl pairs, #2 and #3, are circled in Figure 2a. When the images are compared as a function of Δt, each of these bright spots clearly separates into a pair of easily resolved bright spots.

Line scans along the BBO row containing bright spot #2 are displayed in Figure 2e for $\Delta t = 0$, 21, 35, and 51 min (curves a−d). For $\Delta t = 0$, the line scan has three peaks marking the positions of the three BBO_V's and a fourth, more intense peak marking hydroxyl pair #2. The three BBO_V's remain over the 51-min time scale of this experiment and serve to mark changes in the hydroxyl pair. The full width at half-maximum (fwhm) characterizing the hydroxyl pair along the [001] direction in curve a spans 0.9 nm (BBO's are separated by 0.3 nm), and its maximum is centered between two BBO sites. After 21 min (curve b), two local maxima of equal intensities are resolved and the overall fwhm increases from 0.9 to 1.2 nm. Both peaks are centered on the BBO sites and are separated by 0.6 nm (the spacing between next nearest neighbor BBO's). We interpret the change from curve a to curve b as a hydrogen on either OH_V or OH_B hopping to the adjacent BBO. Comparing the four curves in Figure 2e indicates that, referenced to the BBO_V's, the hydrogens on both OH_V and OH_B hop slowly apart to nearest-neighbor BBO's. While hopping closer together is observed (see below), it is an infrequent event and is not observed in Figure 2e. The two intense maxima in curve d of Figure 2e are interpreted as two hydroxyls separated by three BBO's. The fwhm of each of these peaks is 0.5 nm, significantly less than the 0.9-nm width associated with the nearest-neighbor pair of hydroxyls in curve a.

As noted above, BBO_V's fill slowly. Tracking these as a function of time provides valuable insight, because the positions of the original BBO_V's are known. The BBO_V encircled and labeled #1 in Figure 2a ($\Delta t = 0$) becomes filled in Figure 2b ($\Delta t = 21$ min). Line scans for $\Delta t = 0$, 21, 35, and 51 min are shown in Figure 2f. In curve a ($\Delta t = 0$), five vacancies are located, one of which is altered in curve b. The width of the bright spot in curve b is 0.9 nm, as in curve a of Figure 2e, and the position of the original BBO_V lies to the left-hand side of this intensity distribution. For $\Delta t = 35$ min, curve b, two equal-

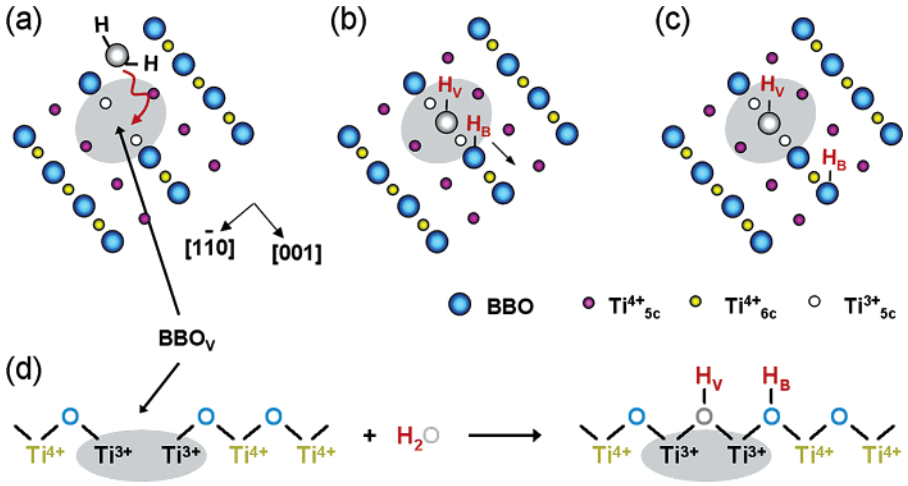

Figure 3. Schematic model of the diffusion process observed in Figure 2: (a) TiO_2(110) surface with BBO_V; (b) pair of hydroxyl groups (OH_B + OH_V) formed after water adsorption and dissociation on BBO_V; (c) separated OH group pair after H_B diffusion; (d) side view of the water reaction with the BBO_V site along the [001] direction. Five-coordinate Ti^{4+} cations are designated Ti^{4+}_{5c}, six-coordinate Ti^{4+} cations by Ti^{4+}_{6c}, and five-coordinate Ti^{3+} cations are designated Ti^{3+}_{5c}. The gray areas highlight the region of interest.

intensity peaks are resolved. Most significantly, one is located at the original BBO_V and the other at the nearest available BBO. For $\Delta t = 51$ min, curve d, there is no change in the line scan.

From the three line scans in Figure 2f, we conclude that the first hydrogen hop occurs for OH_B. Examining first hops in eight independent experiments using only the geminate OH_V-OH_B pairs with known original BBO_V positions (24 of 112 events) shows that 88% (21 of 24 events) result in hydrogen motion from OH_B. That is, the first hop seldom involves motion of the hydrogen of the OH that occupies the original BBO_V (3 of 24 events); rather, the first hydrogen hop occurs predominantly from OH_B, the hydroxyl group formed by adding hydrogen to the nearest BBO during H_2O dissociation at BBO_V. Although the statistical uncertainty is rather large, it is clear that the first hop associated with the nearest-neighbor hydroxyl pair formed from H_2O dissociative adsorption strongly favors motion of the hydrogen on OH_B. This observation is rather puzzling considering the generally accepted view of equivalent OH groups formed by water dissociation. Therefore, we would expect that, upon OH pair formation, the charge should redistribute and lead to formation of a symmetric OH pair. Our experiments clearly indicate that this is not the case and that the electronic environment of these two OH groups is likely different.

Figure 3 is a schematic description of the prevailing sequence of events observed at low water coverages, i.e., water adsorption (Figure 3a), its dissociation into an adjacent OH_V-OH_B pair (Figure 3b), and H_B diffusion (Figure 3c). A side view of H_2O dissociation on a BBO_V site in a BBO row highlighting the presence of two five-coordinated Ti^{3+} ions underneath the BBO_V site before and after the water adsorption is shown in Figure 3d. The fact that the Ti^{3+} defect states remain preserved upon water adsorption is supported by prior spectroscopic investigations.[4,6,8,11] Theoretical calculations suggest that the excess charge associated with the BBO_V's is not localized only on the two Ti^{3+} ions directly underneath the BBO_V but also extends over the neighboring five-coordinated Ti^{4+} ions surrounding the BBO_V site along the [1$\bar{1}$0] direction.[19−21] Nonetheless, the simplified formal charge picture depicted in Figure 3d illustrates the inequivalent charge distribution beneath OH_V and OH_B along the [001] direction. In this picture, the OH_V is surrounded by two Ti^{3+} ions, while the OH_B is surrounded by one Ti^{3+} and one Ti^{4+} ion. We speculate that this difference in the charge density is likely responsible for the difference in the frequencies for H_B and H_V hops leading to the separation of geminate OH_V-OH_B pairs. An alternative explanation involves different binding of the BBO formed by adsorption at the BBO_V. Further theoretical calculations will be critical in addressing this issue.

Since tip-induced effects are common,[22,23] we have taken special care to assess their influence on our experimental findings. Two areas on the same H_2O/TiO_2(110) surface were compared. After the initial scans of both areas, one area was scanned continuously 20 more times ($\Delta t = 50$ min), followed by final scans of both areas. The total number of hops observed after the final scan was compared on both areas. Within statistical uncertainty, the measured hopping rates were the same, indicating that tip effects (e.g., electron and field-induced diffusion) were negligible under our experimental conditions.

We have also considered the effect of local surface environment. We searched for a correlation between the OH_B position with respect to nearby BBO_V's, but no apparent correlation was found, and therefore, we conclude that OH_B appears randomly on either side of OH_V.

Excluding the tip-assisted hydrogen hopping we conclude that the observed diffusion is thermally activated. We have analyzed 112 events in 8 separate experiments and determined hopping rates ranging from 2×10^{-5} to 3×10^{-4} OH^{-1} s^{-1} with an average value of 1×10^{-4} OH^{-1} s^{-1} at the nominal temperature of 300 K. The large span of the hopping rates from experiment to experiment is attributed to slight temperature differences. Although the temperature is near 300 K in every case, the clean substrate was moved to the STM from the preparation manipulator as the indicated temperature reached 350−320 K during cooling to limit background water adsorption.

Assuming an Arrhenius-type process, the temperature dependence of the hopping rate, r, can be written as

$$r = \nu_0 \exp(-\Delta E_B/k_B T) \qquad (1)$$

where ν_0 is the attempt frequency, k_B the Boltzmann constant, and ΔE_B the activation energy barrier associated with the hop. Typically, the values of attempt frequencies are comparable to stretching-mode frequencies of the adsorbate and are normally on the order of 10^{13} s^{-1}.[24] We use this value to estimate the activation barrier for the first hydrogen hop from OH_B along the BBO row to be $\sim 1.0 \pm 0.03$ eV. This value can be compared with a previously calculated energy barrier for hydrogen hopping along the BBO row of ~ 1.5 eV.[15] Since the value of ν_0 is unknown, this comparison should not be considered quantitative.

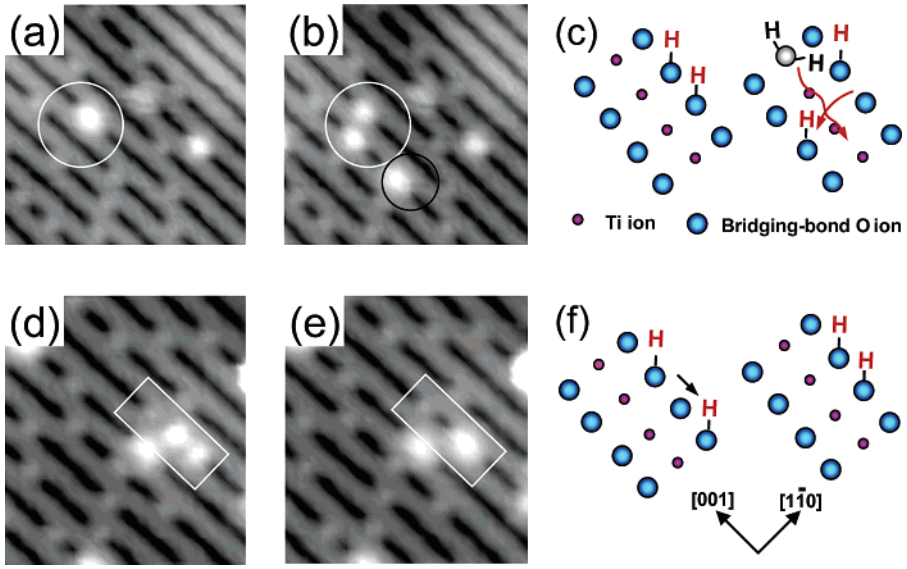

Figure 4. (a−c) An example of observed cross-row diffusion of hydrogen from hydroxyl pair[15] assisted by molecular H_2O diffusion along a Ti^{4+} row as documented by the presence of a new water molecule adsorbed in the vicinity: (a,b) two sequential STM images; (c) schematic model of water-assisted cross-row diffusion. (d−f) An example of two separated hydroxyl groups originating from the same water molecule diffusing closer together: (d,e) two sequential STM images; (f) schematic model of H diffusion.

Nonetheless, due to expected repulsion between the hydrogen pairs, one can speculate that the ΔE_B value determined for the first hop is smaller than the value of the diffusion barrier for isolated hydrogens. This is supported by previous calculations that show that the binding energy for isolated OH is 0.15 eV higher compared to paired OH groups.[14] To confirm this difference experimentally, hopping rates for the second and consecutive hops have to be measured. Several such events were presented in Figure 2. Unfortunately, our current experiments, conducted close to the ambient temperature, did not allow us to obtain a sufficient data sample to extract statistically meaningful hopping rates for OH groups separated by bare BBO sites. Our future experiments are focusing on STM imaging at elevated temperatures and should provide a more complete map of the potential energy landscape governing hydrogen motion on TiO_2(110).

If we use the experimentally determined hopping rates combined with the average value for an activation barrier of 1.0 ± 0.03 eV, we can estimate the likely experiment-to-experiment temperature variations across the STM data sets to be only ±7 K, well within expectations based on the employed experimental procedure (see above).

Besides the predominant event, hydrogen hopping of OH_B, other minority events were also observed. The previously reported H_2O-assisted hydrogen hopping from one BBO row to another[15] is shown in Figure 4a−c. At the very low H_2O coverages (<1.5%) employed here, this event is rather uncommon (observed only 8 times in 112 events).

In image Figure 4a, the fwhm of the circled bright spot is 0.9 nm, identifying it as a hydroxyl pair. Later (Δt = 11 min; Figure 4b), this hydroxyl pair appears as two hydrogens (0.5 nm fwhm) located on adjacent rows, with one hydrogen located at the position of the original pair. In this case, the OH diffusion is assisted by H_2O that adsorbs near the OH pair and, as diagrammed in Figure 4c, diffuses along the adjacent Ti^{4+} row past the OH pair, transiently forming H_3O^+, depositing one of the three available hydrogens on an adjacent row, and then undergoing trapping and dissociation at a nearby vacancy (i.e., the OH pair in Figure 4b that is marked with a black circle). In other experiments where more than 2.0% of the BBO_V's were filled with hydroxyls, the cross-row hopping probability increased to 18% of the total number of hops (82% along the rows). We presume this results from an increased probability of adsorbed H_2O passing one or more OH_B species and assisting row hopping before dissociating at a vacancy. These results agree with earlier work[15] that row hopping is more likely at higher water coverages when most of the BBO_V's are filled with OH groups.

Another rare event involves two OH's separated by a BBO moving toward each other (observed only 3 times in 112 events) as illustrated in Figure 4d,e and shown schematically in Figure 4f. Comparing the hydroxyl positions in the rectangle of Figure 4d,e, we observe hydrogen hopping from the upper left OH group toward the lower right OH group. As expected for hydroxyl groups separated by one or more BBO's, the fwhm of the two peaks in Figure 4d is 0.5 nm (line profile not shown). In Figure 4e, the fwhm of the single bright spot is 0.9 nm, consistent with a nearest-neighbor pair of OH groups. For pairs with one BBO between the hydroxyls (as in Figure 4d) the probability of hopping apart by one additional BBO (two BBO's between hydroxyls) is approximately 35 times more likely than hopping toward each other, i.e., the energy barrier for moving further apart is somewhat lower than that for moving closer together. The repulsive interaction between two hydrogens is not surprising. This is in agreement with theoretical calculations by Wendt et al.[14] where the binding energy of two neighboring OH groups has been computed to be 0.15 eV lower compared to that of two isolated OH groups. While the separation range over which this difference exists cannot be deduced from the present experiments, we hypothesize that the two OH's likely become independent when more than two BBO's separate the two hydroxyls. If this is the case, the probability of hopping toward and away would become equal.

4. Conclusions

Using in situ scanning tunneling microscopy, we imaged the dissociation of water and the diffusion dynamics of dissociation products at coverages lower than the vacancy concentration, i.e., no Ti^{4+}-bonded water molecules on the surface. Our results confirm that paired hydroxyl groups are the direct product of water dissociation on oxygen vacancies. For the first time, the

hydrogens of these hydroxyl pairs are found spontaneously separated along the (001) direction, indicating hydrogen hopping without the assistance of water molecules. Importantly, it is found that the hydrogens of the hydroxyl pair are not identical; the first hydrogen hop is much less likely for the hydrogen located at the original vacancy.

Acknowledgment. This work was supported by the U.S. Department of Energy Office of Basic Energy Sciences, Chemical Sciences and Materials Sciences Divisions, Robert A. Welch Foundation (F-0032), and National Science Foundation (CHE-0412609), and performed at W. R. Wiley Environmental Molecular Science Laboratory, a national scientific user facility sponsored by the Department of Energy's Office of Biological and Environmental Research located at Pacific Northwest National Laboratory (PNNL). PNNL is operated for the U.S. DOE by Battelle under contract no. DE-AC06-76RLO 1830. We would like to thank M.A. Henderson (PNNL) for stimulating discussions.

Supporting Information Available: Journal cover art of the three-dimensional scanning tunneling microscopy images and schematic views of the TiO_2(110) surface before and after water adsorption and dissociation. Preferential diffusion of the hydrogen that split off from OH demonstrates the inequivalence of the two geminate OH groups. This material is available free of charge via the Internet at http://pubs.acs.org.

References and Notes

(1) Thompson, T. L.; Yates, J. T. *Top. Catal.* **2005**, *35*, 197.
(2) Gratzel, M. *Nature (London)* **2001**, *414*, 338.
(3) Fujishima, A.; Honda, K. *Nature (London)* **1972**, *238*, 37.
(4) Diebold, U. *Surf. Sci. Rep.* **2003**, *48*, 53.
(5) Henderson, M. A. *Surf. Sci. Rep.* **2002**, *46*, 5.
(6) Kurtz, R. L.; Stockbauer, R.; Madey, T. E.; Roman, E.; Desegovia, J. L. *Surf. Sci.* **1989**, *218*, 178.
(7) Henderson, M. A. *Surf. Sci.* **1996**, *355*, 151.
(8) Henderson, M. A.; Epling, W. S.; Peden, C. H. F.; Perkins, C. L. *J. Phys. Chem. B* **2003**, *107*, 534.
(9) Hugenschmidt, M. B.; Gamble, L.; Campbell, C. T. *Surf. Sci.* **1994**, *302*, 329.
(10) Brookes, I. M.; Muryn, C. A.; Thornton, G. *Phys. Rev. Lett.* **2001**, *87*, 266103.
(11) Krischok, S.; Hofft, O.; Gunster, J.; Stultz, J.; Goodman, D. W.; Kempter, V. *Surf. Sci.* **2001**, *495*, 8.
(12) Schaub, R.; Thostrup, R.; Lopez, N.; Laegsgaard, E.; Stensgaard, I.; Norskov, J. K.; Besenbacher, F. *Phys. Rev. Lett.* **2001**, *87*, 266104.
(13) Suzuki, S.; Fukui, K.; Onishi, H.; Iwasawa, Y. *Phys. Rev. Lett.* **2000**, *84*, 2156.
(14) Wendt, S.; Schaub, R.; Matthiesen, J.; Vestergaard, E. K.; Wahlstrom, E.; Rasmussen, M. D.; Thostrup, P.; Molina, L. M.; Laegsgaard, E.; Stensgaard, I.; Hammer, B.; Besenbacher, F. *Surf. Sci.* **2005**, *598*, 226.
(15) Wendt, S.; Matthiesen, J.; Schaub, R.; Vestergaard, E. K.; Laegsgaard, E.; Besenbacher, F.; Hammer, B. *Phys. Rev. Lett.* **2006**, *96*, 066107.
(16) Bikondoa, O.; Pang, C. L.; Ithnin, R.; Muryn, C. A.; Onishi, H.; Thornton, G. *Nat. Mater.* **2006**, *5*, 189.
(17) Zhang, Z.; Bondarchuk, O.; White, J. M.; Kay, B. D.; Dohnálek, Z. *J. Am. Chem. Soc* **2006**, *128*, 4198.
(18) http://www.nanotec.es.
(19) Vijay, A.; Mills, G.; Metiu, H. *J. Chem. Phys.* **2003**, *118*, 6536.
(20) Li, B.; Zhao, J.; Onda, K.; Jordan, K. D.; Yang, J. L.; Petek, H. *Science* **2006**, *311*, 1436.
(21) Rasmussen, M. D.; Molina, L. M.; Hammer, B. *J. Chem. Phys.* **2004**, *120*, 988.
(22) Fomin, E.; Tatarkhanov, M.; Mitsui, T.; Rose, M.; Ogletree, D. F.; Salmeron, M. *Surf. Sci.* **2006**, *600*, 542.
(23) Dulot, F.; Eugene, J.; Kierren, B.; Malterre, D. *Appl. Surf. Sci.* **2000**, *162*, 86.
(24) Barth, J. V.; Brune, H.; Fischer, B.; Weckesser, J.; Kern, K. *Phys. Rev. Lett.* **2000**, *84*, 1732.